DIAGNOSTIC NUCLEAR MEDICINE

In Vivo Assessment of Phagocytic Properties of Kupffer Cells

S. N. Reske, K. Vyska, and L. E. Feinendegen

Institute of Medicine, Nuclear Research Center Jülich, West Germany

Three-compartment analysis was used to assess the kinetics of phagocytosis of Tc-99m-labeled human serum albumin microparticles (Tc-99m HSA-MM) in human Kupffer cells in vivo. The tracer turnover in these phagocytic cells could be described by a monoexponential accumulation with a two-stage elimination phase. Three-compartment analysis of the Tc-99m HSA-MM kinetics allowed us to quantify tracer attachment, phagocytosis, and degradation in Kupffer cells. The calculated time course of phagocytosis in ten control subjects proved to be identical to that of phagocytosis of various test substances in mouse macrophage monolayers (*1*). In addition, an impairment of particle turnover at the macrophage membrane, a significantly diminished ($p < 0.01$) phagocytosis rate of the tracer, was observed in ten patients with various tumors.

J Nucl Med 22: 405–410, 1981

The interaction of microparticles with macrophages in tissue culture has been characterized (*2–4*) as a three-stage process: (a) attachment at the receptor of the macrophage membrane, (b) phagocytosis, and (c) intralysosomal degradation of the engulfed material.

To evaluate macrophage functions in vivo, clearance rates of inert test colloids from peripheral blood were determined in patients (*5–10*). However, blood clearance might be considerably influenced by the complex distribution of the test material and the heterogeneity of the macrophage populations (*11*). Colloid clearance rates, therefore, rather indicate an ill-defined global RES function and are not conclusive in assessing parameters of phagocytic activity of macrophages (*11*).

Since the only phagocytic cells of the liver's sinusoids are Kupffer cells (*12*), which extract 80–90% of microparticles per blood passage (*5*), externally registered time-activity curves over the liver after injection of radioactively labeled biodegradable colloids reflect turnover of test particles in this cell population. Moreover, specific parameters of the Kupffer cell can be obtained by the analysis of the tracer's elimination from the liver.

Received Aug. 28, 1980; revision accepted Nov. 6, 1980.

For reprints contact: L. E. Feinendegen, MD, Institute of Medicine, Nuclear Research Center, Jülich, F.R.G.

MATERIAL AND METHODS

Test colloid. Commercially available Tc-99m-labeled serum albumin microparticles* (Tc-HSA-MM), a degradable tracer, was used as a test colloid (*13*). Ninety percent of the particles range between 0.5 and 2.0 μm, with 1.3×10^8 particles per mg protein. The labeling yield was at least 95% (*13*).

Stringent quality control was assured in each batch of Tc-HSA-MM by scanning electron microscopy (Fig. 1) and dialysis of the labeled particles (*14*). Dialyzable activity after a 90-min incubation period in human serum at room temperature was (2.0 ± 0.75)% (mean ± s.e.m.) of the total activity of the Tc-HSA-MM suspension. The labeled particles were injected i.v. within 90 min after reconstitution of the test kit with pertechnetate (Tc-99m).

Controls. Four male and six female subjects with sporadic nontoxic goiter (mean age 52 yr, range 35–72) were considered as a control population, since in previous studies (*15*) no significant difference in Tc-HSA-MM turnover could be found between patients with sporadic nontoxic goiter and six healthy volunteers. In the controls and in tumor patients the following data were obtained: blood smear, differential count, erythrocyte sedimentation rate, transaminases, alkaline phosphatase, serum protein, serum electrophoresis, and carcinoembryonic

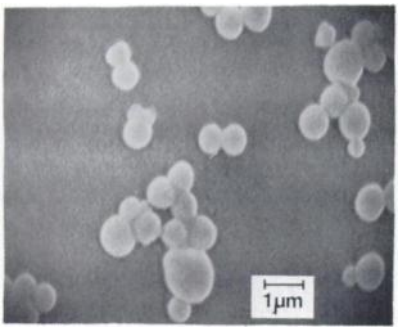

FIG. 1. Scanning electron micrograph of Tc-HSA-MM; × 10,000.

antigen. In the control population all these parameters were in the normal range.

Patients. Ten patients with malignancies (six male, four female) with a mean age of 55 yr (range 35–70) were classified according to the histological type of disease and clinical status according to the TNM classification (*17*) of the Union International Contre Cancer (UICC) (Table 1). On the basis of the clinical status and the serological and scintigraphic findings, there was no evidence of liver invasion by the primary tumor, liver metastases, or inflammatory liver disease. All patients were examined before the beginning of curative or adjuvant therapy.

Patient examination. Two millicuries Tc-HSA-MM (0.02 mg/kg body weight) were injected i.v. as a bolus. The radioactivity distribution in the lower thorax and upper abdomen was recorded with a large-field gamma camera in anterior projection. The frame rate was one frame per 15 sec, the registration time 90 min. In control subjects, serial blood samples (2 ml) were obtained and dialyzed against phosphate-buffered saline (PBS) at room temperature. Tc-HSA-MM were isolated from peripheral blood samples by centrifugation in microcapillaries in sodium metrizoate† at 3000 *g* (*14*).

TABLE 1. DIAGNOSIS AND TNM CLASSIFICATION OF TUMOR PATIENTS

Patient	Diagnosis	TNM classification
F.K.	Breast ca	T2, N2b, M1C2
K.D.	Breast ca	T2, N1b, M1
A.N.	Breast ca	T1a, N3b, M1C2
P.H.	Prostate ca	T3-4, NX, M1C2
D.B.	Hodgkin Amyloidosis	III B
P.S.	Non-Hodgkin Lymphoma	III
H.A.	Thyroid ca (Struma maligna langhans)	r T1, NO, MQ
N.C.	Bronchial ca (adeno-ca)	T2, NO, MO
Sch.P.	Bronchial ca (small cell ca)	T1, NO, MO
P.E.	Colon ca (sigmoid)	T3a, N1, MX

TABLE 2. SLOPES FOUND BY COMPUTER APPROXIMATION OF TIME-ACTIVITY CURVES (ROI-LIVER) IN 10 CONTROL PERSONS AND 10 TUMOR PATIENTS

Control Subjects			
Patient	g_1	g_2	g_3
E.L.	0.371	0.156	0.00459
M.B.	0.369	0.109	0.003
K.A.	0.502	0.156	0.000852
N.R.	0.341	0.157	0.00251
P.B.	0.306	0.135	0.0032
J.H.	0.472	0.103	0.00244
R.S.	0.277	0.126	0.0032
K.N.	0.381	0.139	0.0031
D.H.	0.402	0.110	0.0020
J.O.	0.350	0.138	0.0025
$\bar{x}$ ± s.d.	0.377 ± 0.069	0.133 ± 0.02	0.0027 ± 0.00096
Tumor patients			
	g_1	g_2	g_3
P.H.	0.41	0.143	0.0013
F.K.	0.529	0.083	0.00265
U.D.	0.402	0.100	0.00138
D.B.	0.387	0.0017	0.00011
A.N.	0.571	0.096	0.002
P.S.	0.684	0.075	0.0012
H.A.	0.642	0.0109	0.00013
N.C.	0.642	0.0247	0.00219
P.E.	0.521	0.0707	0.00087
Sch.P.	0.604	0.0654	0.00164
$\bar{x}$ ± s.d.	0.54 ± 0.11	0.067 ± 0.044	0.00135 ± 0.00087

Data evaluation. A region of interest was selected over the right lobe of the liver. The time-activity curve obtained over this ROI (Fig. 3) was fitted with three exponential functions by a computer program that optimized the approximations. The slope (g_1) and intercept (J_1) for the accumulation phase of the turnover curve were determined, as well as the slopes and intercepts for the fast (g_2, J_2) and slow (g_3, J_3) components of the elimination phase.

By 4 min after the injection, ~65% of Tc-HSA-MM is located in the liver, whereas ~35% is found in peripheral blood. The background due to radioactivity in the liver's sinuosoidal blood volume was estimated as <3% of the radioactivity bound to the Kupffer cells, and can therefore be neglected. For this estimate the total blood volume was taken as 5000 ml, the liver sinusoidal blood volume 300 ml (*16*), and the Tc-HSA-MM blood-clearance rate constant 0.35/min (see Table 2).

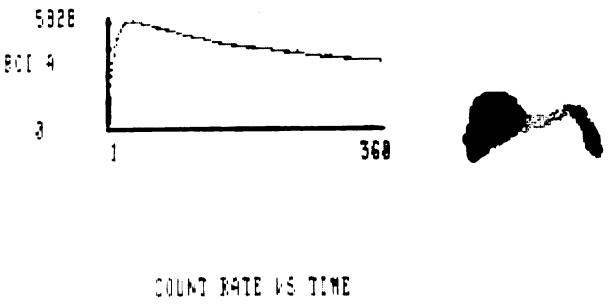

FIG. 2. Time-activity curve registered over liver ROI of control subject after i.v. bolus injection of 2.0 mCi Tc-HSA-MM.

RESULTS

Curve parameters. Figure 2 shows a time-activity curve registered over the liver ROI in a normal person after i.v. injection of Tc-HSA-MM. The curve has a steep upslope and a two-phase elimination period. The computer-fitted curve is shown in Fig. 3. Tracer accumulation shows a monoexponential upslope (g_1 = 0.377/min) whereas its elimination period can be described by two components (g_2 = 0.133/min, g_3 = 0.027/min, Table 2), suggesting a particle turnover controlled by at least three time-limiting processes.

The blood clearance and the time-activity curves for dialyzable activity obtained in five normals (Fig. 4) indicate: (a) a fast clearance of Tc-HSA-MM from peripheral blood; (b) a coincidence between the increasing dialyzable activity between 4 and 30 min in peripheral blood and the fast elimination component of the ROI turnover curve; and (c) the relatively constant concentration of dialyzable activity in peripheral blood between 30 and 90 min, which indicates a steady state of production and disposal of dialyzable Tc-99m activity. Figure 4 also shows the clearance of Tc-HSA-MM isolated from peripheral blood of five control subjects.

Compartmental model. On the basis of the principal characteristics of the interaction of particulate material with macrophages (i.e., attachment, phagocytosis, digestion) (*2,4,11,12,18*) a three-compartment model was proposed for the pharmacokinetics of Tc-HSA-MM

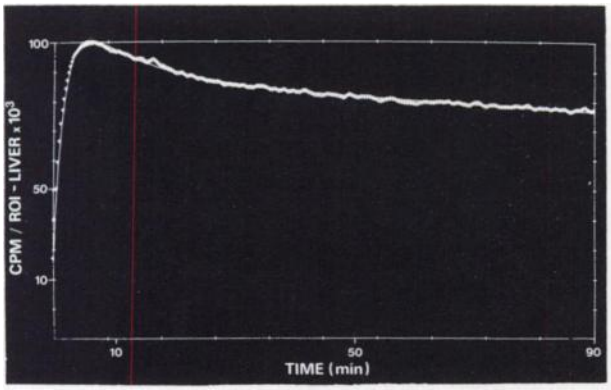

FIG. 3. Computer approximation of time-activity curve from liver ROI.

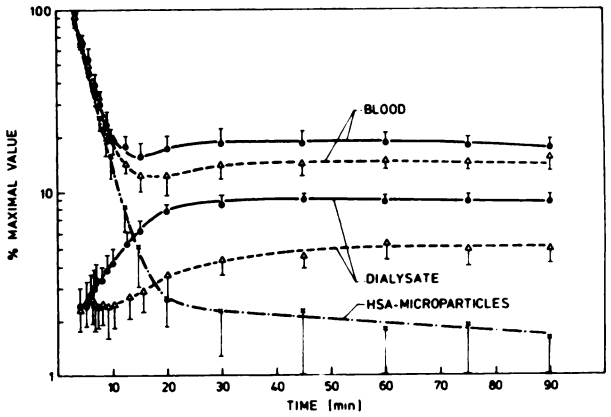

FIG. 4. Time course of radioactivity in blood and dialysate in control subjects (●) and tumor patients (Δ), and blood clearance curve of Tc-HSA microparticles (x).

(Fig. 5). Compartment 1 describes the particle distribution pool, with g_1 the slope of the curve for particle clearance from the circulation. Compartment 2 was considered to reflect the particle turnover at the macrophage membrane, with a two-way flow of activity: (a) backflow of dialyzable activity into the circulation, and (b) phagocytosis of the bulk of the membrane-bound activity. Compartment 3 was related to the intracellular space of the Kupffer cells, and reflects the time course of phagocytosis and subsequent metabolic degradation of the colloid. Assuming first-order kinetics for the particle transport (*20*) and that the turnover curve obtained over the liver ROI is the sum of the membrane-associated and the intracellular bound activity, the constants k_{21}, k_{02}, k_{32}, and k_{03} were calculated as described in the Appendix. Figure 6 shows typical calculated time-activity curves in Compartments 1, 2, and 3, obtained in a normal person (fine curves) and, for comparison, in a tumor patient (heavy curves). The rate constants found in ten control persons are summarized in Table 3.

In tumor patients, marked changes of Tc-HSA-MM turnover are observed (Table 2). The steeper slope (g_1) indicates an accelerated Tc-HSA-MM clearance from

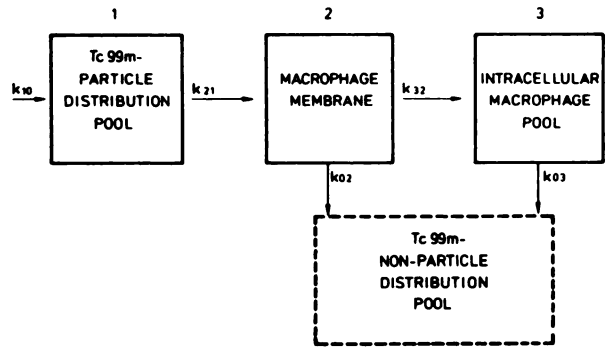

FIG. 5. Compartmental model for Tc-HSA-MM disposition in v. Kupffer cells.

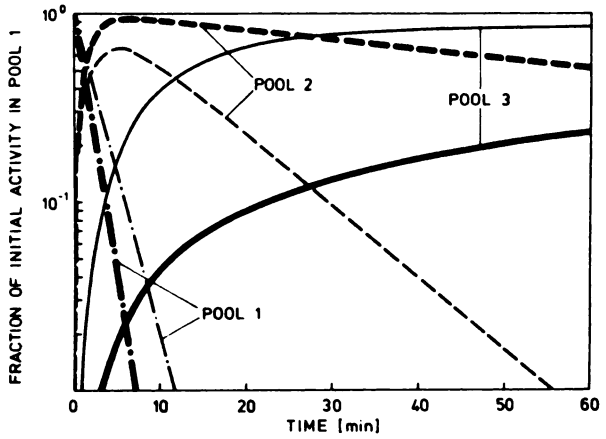

FIG. 6. Calculated time-activity curves in Pools 1, 2, and 3 in representative control subject (light curves) and a tumor patient (heavy curves).

the circulation. Constants g_2 and g_3, characterizing the elimination of Tc-HSA-MM from the liver, are diminished compared with controls. The constant k_{32} (characterizing phagocytosis) as well as k_{02} and k_{03} (characterizing extracellular and intracellular Tc-HSA-MM decomposition) were reduced. Tc-HSA-MM turnover in Pool 2 and invasion into Pool 3 were markedly retarded (Fig. 6). A retarded and diminished reappearance of dialyzable activity in the peripheral blood of tumor patients was observed (Fig. 4).

TABLE 3. RATE CONSTANTS OF THE THREE-COMPARTMENT MODEL IN 10 CONTROL SUBJECTS AND 10 TUMOR PATIENTS

Control Subjects				
Patient	k_{21}	k_{32}	k_{02}	k_{03}
E.L.	0.371	0.1084	0.0476	0.00459
M.B.	0.369	0.0859	0.0231	0.003
K.A.	0.502	0.145	0.0113	0.000852
N.R.	0.341	0.133	0.0235	0.00251
P.B.	0.306	0.111	0.0169	0.0032
J.H.	0.472	0.0825	0.0205	0.00244
R.S.	0.277	0.0993	0.0267	0.0032
K.N.	0.381	0.113	0.026	0.0031
D.H.	0.402	0.0891	0.021	0.0020
J.O.	0.350	0.115	0.017	0.0025
$\bar{x} \pm$ s.d.	0.377 ± 0.069	0.108 ± 0.02	0.0233 ± 0.01	0.0027 ± 0.00096
Tumor Patients				
	k_{21}	k_{32}	k_{02}	k_{03}
P.H.	0.41	0.1346	0.0084	0.0013
K.D.	0.529	0.066	0.017	0.00265
D.B.	0.402	0.0853	0.0147	0.00138
A.N.	0.387	0.0016	0.00011	0.00011
P.S.	0.571	0.069	0.027	0.002
H.A.	0.684	0.062	0.013	0.0012
N.C.	0.642	0.00541	0.00549	0.00013
P.E.	0.642	0.0157	0.009	0.00219
F.K.	0.521	0.059	0.0117	0.00087
Sch.P.	0.604	0.0512	0.0142	0.00164
$\bar{x} \pm$ s.d.	0.54 ± 0.11	0.055 ± 0.04	0.0121 ± 0.0072	0.00135 ± 0.00083

DISCUSSION

The analysis of externally registered time-activity curves from an hepatic ROI after application of Tc-99m-labeled biodegradable microparticles revealed three slopes, g_1, g_2, and g_3, varying only in narrow ranges in control subjects. This finding indicates an interaction of Tc-99m-labeled microparticles with Kupffer cells controlled by at least three time-dependent processes, and it fits well to the three-stage process of microparticle endocytosis found in vitro (*2,4,11,12,18*): attachment of microparticles at the macrophage membrane, phagocytosis, and biodegradation. Taking into account this three-stage process, we have proposed a three-compartment model for the turnover of Tc-HSA-MM in Kupffer cells (*19*), which allows global quantitation of microparticle transport in these cells.

The accumulation of tracer in the liver is characterized by k_{21}, which might be influenced by the liver's sinusoidal blood flow (*23*), the in vivo opsonisation of the test particles (*22*), the test-particle surface, the number and density of receptor sites at the Kupffer-cell membrane (*24,25*), the number and phagocytic capacity of the Kupffer cells, and also of the function of the entire body RES. This k_{21}, therefore, as obtained from the hepatic turnover curve, does not specifically describe the phagocytic activity of Kupffer cells.

The elimination of tracer from the liver, however, can be expected to describe a specific Kupffer-cell function, since biodegradation of Tc-HSA-MM, characterized by g_2 and g_3, is diminished by a factor of at least three compared with the transport of radioactivity from the liver. The latter is governed mainly by the sinusoidal blood flow, which can be characterized by a value at least close to that of g_1.

The particle turnover at the macrophage membrane (Compartment 2) was considered as a two-way flow of activity. First, decomposition and backflow of dialyzable activity into the circulation (characterized by k_{02}), resulting in a significant rise of dialyzable blood activity (Fig. 4), which exceeds the activity released by passive diffusion during dialyses of Tc-HSA-MM in vitro (*14*). Release of dialyzable activity therefore seems to be caused by an active metabolic process occurring during the transport of Tc-HSA-MM across the macrophage membrane, possibly caused by proteases secreted by macrophages during phagocytosis (*26*). Second, phagocytosis of microparticle-bound activity, characterized by k_{32}. The in vivo determination of phagocytic properties of Kupffer cells might be hampered, however, by

several factors, for example in vivo opsonic activity of the patient's serum (*22*), enzyme activity of blood and tissue fluid (*18*), functional heterogeneity of phagocytic cells (*11,18*), and extrahepatic determination of hepatic curve parameters without allowance for Tc-HSA-MM not associated with macrophages or for its metabolic activity. Interestingly enough, however, the time course of phagocytosis of Tc-HSA-MM in vivo, as predicted by the model, is in good agreement with the time course of phagocytosis determined in vitro in macrophage monolayers using C-14-labeled tubercle bacilli or starch-gel particles as test substances (*1*).

Tracer elimination from Compartment 3 (characterized by k_{03}) was considered to reflect the half-life (~4 hr) of proteolysis and backflow of degradation products of Tc-HSA-MM from the Kupffer cells in control subjects. This is shorter than the half-life of 8–48 hr observed for proteolysis of I-125-labeled antigen-antibody complexes in macrophage monolayers (*27*) and might be explained by noncovalent surface labeling of the preformed globular test colloid.

In tumor patients, the kinetics of Tc-HSA-MM was changed: Though k_{21} indicated an accelerated clearance of tracer from the circulation, microparticle transport across the macrophage membrane—and accordingly phagocytosis—were markedly delayed. Release of dialyzable activity into the blood (Fig. 4) was also delayed and diminished. Since no liver metastases or direct tumor invasion into the liver could be detected, interaction of Kupffer cells with products of tumor origin might be postulated. Modulation of lymphoreticular cell functions by tumors has been shown in experimental animals as well as in man (*28*). Potential modulating products of tumor origin are prostaglandins, chemotactic factors, immunosuppressive peptides (*30,28*), membrane glycoproteins (*29*), tumor antigens, antigen-antibody complexes (*30*), and cell-directed inhibitor (CDI) (*31*). CDI has also been shown to suppress the phagocytic response of neutrophils (*31*). Thus impaired phagocytic properties of Kupffer cells might reflect a modulation of the immune status of these patients. Further studies should clarify the interrelationship between stage and biological behavior of neoplasms, immune status, and Kupffer-cell function.

CONCLUSIONS

1. Tc-99m microparticles offer a suitable tracer for the evaluation of Kupffer-cell function in vivo.
2. Three-compartment analysis of Tc-HSA-MM turnover allows quantitation of in vivo Kupffer-cell functions in man.
3. In all tumor patients examined, a greatly reduced phagocytosis of particles is observed.

FOOTNOTES

* TcK-9, Isotopen-Dienst West GmbH, Dreieich, FRG.

† Isopaque, 1, 13 w/v, Deutsche Pharmacia GmbH, Freiburg, FRG.

APPENDIX

The solutions of a system of equations describing an unrestricted three-compartment system (*30*) can be written as

$$\text{Compartment 1: } \frac{q_1(t)}{q_{10}} = \frac{R_1(t)}{R_{10}} = H_1 \cdot e^{-g_1 \cdot t} = 1.0 \cdot e^{-g_1 \cdot t},$$

$$\text{Compartment 2: } \frac{q_2(t)}{q_{10}} = \frac{R_2(t)}{R_{10}} = K_1 \cdot e^{-g_1 \cdot t} + K_2 \cdot e^{-g_2 \cdot t},$$

$$\text{Compartment 3: } \frac{q_3(t)}{q_{10}} = \frac{R_3(t)}{R_{10}} = L_1 \cdot e^{-g_1} + L_2 \cdot e^{-g_2 \cdot t} + L_3 \cdot e^{-g_3 \cdot t};$$

where $q_x(t)/q_{10}$ is the fraction of dose, q_{10}, in compartment x; $R_x(t)/R_{10}$ are arbitrary units of count rates of a radiation detector looking at compartment x; and g_i, H_i, k_i, and L_i are the slopes and normalized intercepts of curves for quantity of tracer in the i^{th} compartment. It is assumed that the contribution of Compartment 1 to the hepatic turnover curve is negligible. Thus the equation for the hepatic turnover curve is given by

$$R_{ROI}(t) = (K_1 + L_1) \cdot e^{-g_1 \cdot t} + (K_2 + L_2) \cdot e^{-g_2 \cdot t} + L_3 \cdot e^{-g_3 \cdot t}.$$

The following hepatic parameters can be calculated from slopes (g_i) and intercepts (J_i) of the ROI turnover curve:

1. Turnover rate constants:

$$k_{32} = \frac{(g_3 - g_1)(g_2 - g_3)(A + 1)}{A(g_3 - g_1) - g_2 + g_3}$$

$$k_{02} = g_2 - k_{32},$$

$$k_{21} = g_1,$$

$$k_{03} = g_3;$$

where

$$A = \frac{J_1}{J_2} = \frac{K_1 + L_1}{K_2 + L_2},$$

and J_i is the i^{th} intercept of the ROI turnover curve.

2. Intercepts: $K_1 = \dfrac{g_1}{g_2 - g_1}$

$$K_2 = -K_1$$

$$L_1 = k_{32} \cdot K_1 \cdot \frac{1}{(g_3 - g_1)}$$

$$L_2 = k_{32} \cdot K_1 \cdot \frac{(-1)}{(g_3 - g_2)}$$

$$L_3 = k_{32} \cdot \frac{g_1}{(g_3 - g_1) \cdot (g_3 - g_2)}$$

REFERENCES

1. KARNOVSKY ML, LAZDINS J, SIMMONS SR: Metabolism of activated mononuclear phagocytes at rest and during phagocytosis. In *Mononuclear Phagocytes*. van Furth R, Ed. Oxford, Blackwell Scientific Publ., 1975, pp 423-437
2. RABINOVITCH M: Phagocytic recognition. In *Mononuclear Phagocytes*. van Furth R, Ed. Oxford, Blackwell Scientific Publ. 1975, pp 299-313
3. COHN ZA: Endocytosis and intracellular digestion. In *Mononuclear Phagocytes*. van Furth R, Ed. Blackwell Scientific Publ. Oxford, 1975, pp 121-128

4. SILVERSTEIN SC, STEINMAN RM, COHN ZA: Endocytosis. *Ann Rev Biochem* 46:669-722, 1977
5. BIOZZI G, BENACERRAF B, HALPERN BN, et al: Exploration of the phagocytic function of the reticuloendothelial system with heat denatured human serum albumin labelled with I^{131} and application to the measurement of liver blood flow, in normal man and in some pathologic conditions. *J Lab Clin Med* 51:230-239, 1958
6. SHEAGREN JN, BLOCK JB, WOLFF SM: Reticuloendothelial system phagocytic function in patients with Hodgkin's disease. *J Clin Invest* 46:855-862, 1967
7. TAPLIN GV: Dynamic studies of liver function with radioisotopes. In *Dynamic Studies With Radioisotopes in Medicine*. Hofer R, Ed. Vienna, IAEA, 1971, pp 373-392
8. BASES RE, KRAKOFF JH: Enhanced reticuloendothelial activity in myeloproliferative disease. *J Reticuloendothel Soc* 2:1-7, 1965
9. MAGAREY CJ, BAUM M: Reticulo-endothelial activity in humans with cancer. *Br J Surg* 57:748-752, 1970
10. SALKY NK, DI LUZIO NR, LEVIN AG, et al: Phagocytic activity of the reticuloendothelial system in neoplastic disease. *J Lab Clin Med* 70:393-403, 1967
11. CARR J: *The Macrophage*. London, Academic Press, 1973, pp 71-72
12. WISSE E: *Kupffer Cells and Other Liver Sinusoidal Cells*. Wisse E, Knook DL, Eds. Amsterdam, Elsevier/North Holland Biomedical Press, 1977, pp 33-60
13. Product Information, Human Serum Albumin Millimicrospheres Kit (Tck-9), CJS, Serin Biomedica, Saluggia (Vercelli) Italia, May, 1978
14. RESKE SN, VYSKA K, HÖCK A, et al: Untersuchung zur nuklearmedizinischen Funktionsprüfung des RES und der unspezifischen Immunabwehr, Der Nuklearmediziner, 2: 144-150, 1978
15. RESKE SN, HÖCK A, VYSKA K, et al: Tc-99m- and I-131-Labelled human serum albumin millimicrospheres for measuring the function of the reticuloendothelial system. In *Nuklearmedizin*. Woldring M, Schmidt HAE, Eds. Stuttgart-New York, Schattauer, 1978, pp 836-839
16. FOLKOW B, NEILE E: *Circulation*. London, Oxford University Press, 1971, pp 484-490
17. HARMER M: *TNM Classification of Malignant Tumors*. 3rd ed., 1978
18. VAN FURTH R, VAN ZWET TL, LEITH PCJ: In vitro determination of phagocytosis and intracellular killing by polymorphonuclear and mononuclear phagocytes. In *Handbook of Experimental Immunology*. Vol. 2, Weir DM, Ed. Oxford, Blackwell Scientific Publ. 1978, 32.1-32.19
19. RESKE SN, VYSKA K, FEINENDEGEN LE: Kinetics of phagocytosis and proteolytic metabolism in liver macrophages in normal persons and tumor patients. *J Nucl Med* 20:606-607, 1979 (abst)
20. KNUDSON DW, KIJLSTRA A, VAN ES LA: Association and dissociation of aggregated IgG from rat peritoneal macrophages. *J Exp Med* 145:1368-1381, 1977
21. ALGINGER P, HARLIK F, KOKOSCHKA EM, et al: Tc-99m sulfur colloid kinetics in patients with malignant melanoma. Proceedings 2nd World Congress on Nuclear Medicine and Biology, Washington, D.C., 1978, p 29 (abst)
22. STOSSEL PT: Phagocytosis. *N Engl J Med* 290:717-723, 1974
23. DOBSON EL, JONES HB: The behavior of intravenously injected particulate material. Its rate of disappearance from the blood stream as a measure of liver blood flow. *Acta Med Scand* 144:(suppl.)1-71, 1952
24. MUTO M, FUJIDA T: Phagocytic activities of Kupffer cells: a scanning electron microscope study. In *Kupffer Cells and Other Liver Sinusoidal Cells*. Wisse E, Knook DL, Eds. Amsterdam, Elsevier, 1977, pp 109-119
25. MUNTHE-KAAS AC: Endocytosis studies on cultured rat Kupffer cells. In *Kupffer Cells and Other Liver Sinusoidal Cells*. Wisse E, Knook DL, Eds. Amsterdam, Elsevier, 1977, pp 325-332
26. UNANUE ER: The regulation of lymphocyte functions by the macrophage. In *Immunological Review*. Vol. 40, Möller G, Ed. Copenhagen, Munsgaard, 1978, pp 227-255
27. COHN ZA: The role of proteases in macrophage physiology, in proteases and biological control. *Cold Spring Harbor Conferences on Cell Prolieration*. Vol. 2, Reich E, Rifkin PB, Shaw E, Eds. 1975, pp 483-493
28. JAMES K: The influence of tumour cell products on macrophage function *in vitro* and *in vivo*. In *The Macrophage and Cancer*. James K, McBride B, Stuart A, Eds. Dept of Surgery, Univ. of Edinburgh, Medical School, Teviot Place, Edinburgh, 1977, pp 225-246
29. ROOS E, DINGEMANS KP: Phagocytosis of tumor cells by Kupffer cells in vivo and in the perfused mouse liver. In *Kupffer Cells and Other Liver Sinusoidal Cells*. Wisse E, Knook DL, Eds. Amsterdam, Elsevier, 1977, pp 183-190
30. HELLSTRÖM KE, HELLSTRÖM J: Immunologic enhancement of tumor growth. In *Mechanisms of Tumor Immunity*. Green J, Cohen S, McCluskey RT, Eds. New York, John Wiley & Sons, 1977, pp 147-174
31. WARD PA, COHEN S: Regulation of inflammatory responses in neoplastic disease. In *Mechanisms of Tumor Immunity*. Green J, Cohen S, McCluskey RT, Eds. New York, John Wiley & Sons, 1977, pp 305-313
32. SHIPLEY AR, CLARK RE: *Tracer Methods for Vivo Kinetics*. New York, Academic Press, 1972